Pis'ma v ZhETF, vol. 98, iss. 12, pp. 962 – 966

Observation of Zitterbegung in spin-orbit coupled atomic gas

S. Cao[+*×], D.-W. Zhang[+], H. Yan[+], Z.-Y. Xue[+1)]

[+]Laboratory of Quantum Engineering and Quantum Materials, and School of Physics and Telecommunication Engineering, South China Normal University, 510006 Guangzhou, China

[*]College of Sciences, South China Agricultural University, 510642 Guangzhou, China

[×]International Center for Quantum Materials, Peking University, 100871 Beijing, China

Submitted 3 September 2013
Resubmitted 14 November 2013

We show that the dynamics of an interacting atomic gas with light-induced gauge potential can be effectively described by a one-dimensional nonlinear spinor Dirac-type equation. Then, it is possible to observe atomic Zitterbewegung (ZB) with interatomic interaction. Here, the effect of two different kinds of nonlinear interaction, repulsive and attractive, on the ZB, are investigated numerically. Therefore, our proposal provides a more realistic situation in simulating the atomic ZB.

DOI: 10.7868/S0370274X1324020X

The phenomenon of Zitterbewegung (ZB) is predicted for free relativistic electrons in a vacuum [1]. It was later recognized that ZB originates from an interference of electron states with positive and negative energies. For an electron, the frequency of ZB is about 1 MeV and its amplitude is on the order of Compton wavelength. Because of such high frequency and small amplitude, direct experiment observation of the electronic ZB is extremely hard. However, the notion of ZB and the resulting formalism are not peculiar to relativistic quantum dynamics. Some phenomena analogous to ZB underlying the same mathematical model with the Dirac equation, have so far been predicted in a wide variety of quantum and even classical physical systems. These systems includes semiconductor quantum wells [2, 3], trapped ions [4], graphene [5], superconductor [6], acoustic [7], and photonic [8, 9] crystals.

On the other hand, it has been widely accepted that the high degree of controllability in cold atomic system provides a possibility of observing phenomena that are experimentally inaccessible in their original counterpart systems. Recently, the spin-orbit coupling in cold atoms have attracted great attentions both experiment and theoretically [10–17]. In particular, several proposals have been presented to simulate and observe ZB with spin-orbit (SO) coupled ultracold atoms [18–25]. For a practical ultracold atomic gas, the interatomic interaction generally leads to nonlinearities, which may result in many interesting phenomena. However, the effects of nonlinear interactions on the atomic ZB, which is important both theoretically and experimentally, are seldom investigated previously.

In this paper, we first propose a simple scheme to observe large amplitude and long lifetime ZB with SO-coupled cold atoms. The effects of nonlinear interactions on the atomic ZB are then investigated numerically. To be more specifically, we consider two different kinds of nonlinear interactions, i.e. repulsive and attractive interactions. Comparing with the noninteracting cases, the amplitude of the ZB is enhanced by the repulsive interaction, while it damps out more quickly, i.e., it has a shorter lifetime. In contract, the amplitude of ZB is reduced by the attractive interaction, while it damps out more slowly, i.e., it has a longer lifetime. We also find that both the repulsive and attractive interactions almost have no effect on the frequency of the atomic ZB. Therefore, our proposal provides a more realistic situation in simulating the atomic ZB.

We begin with the cold atomic simulation of the spinor Dirac-type equation with tunable parameters. Let us consider the motion of an atomic gas with mass m in the $y-z$ plane, with each atom having a Λ-level structure as shown in Fig. 1. The ground states $|1\rangle$ and $|2\rangle$ are coupled to an excited state $|3\rangle$ through spatially varying laser field, with the corresponding Rabi frequencies $\Omega_1 = \Omega\cos(\kappa_y y)e^{-i\kappa_z z}$ and $\Omega_2 = \Omega\sin(\kappa_y y)e^{i(\pi-\kappa_z z)}$, where $\Omega = \sqrt{|\Omega_1|^2+|\Omega_2|^2}$. As shown in Fig. 1b, the Rabi frequencies Ω_1 and Ω_2 can be realized with a pair of lasers $\Omega_{1\pm} = \frac{1}{2}\Omega\exp[i(-\kappa_z z \pm \pm \kappa_y y)]$ and $\Omega_{2\pm} = \frac{1}{2}\Omega\exp\{i[-\kappa_z z \pm (\kappa_y y + \pi/2)]\}$, respectively, where $\kappa_y = \kappa\cos\varphi$ and $\kappa_z = \kappa\sin\varphi$ with κ being the wave number of the lasers and φ being the

1)e-mail: zyxue@scnu.edu.cn

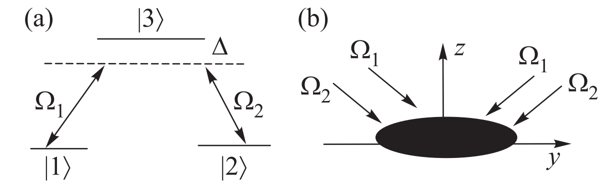

Fig. 1. Schematic illustration of the system. (a) – Atom with a Λ-level configuration interacting with laser beams characterized by Rabi frequencies Ω_1, Ω_2 and a large detunning Δ. (b) – Configuration of laser beams to realize a Dirac-like equation by the lasers Ω_1, Ω_2

angle between the laser and the y axis. The Hamiltonian of a single atom reads $H = \mathbf{P}^2/2m + V(\mathbf{r}) + H_I$, where $V(\mathbf{r}) = \sum_{j=1}^{3}[V_T(\mathbf{r})]|j\rangle\langle j|$ denotes the external potentials and the interaction Hamiltonian is given by $H_I = \hbar\Delta|3\rangle\langle 3| - (\sum_{j=1}^{2}\hbar\Omega_j|3\rangle\langle j| + \text{h.c.})$, with Δ being the detuning. Diagonalizing H_I yields the eigenvalues of $\hbar\{[\Delta - \sqrt{\Delta^2+4\Omega^2}]/2, 0, [\Delta + \sqrt{\Delta^2+4\Omega^2}]/2\}$. Here, we deal the Hamiltonian with the rotating-wave approximation, which just introduces negligible small error. In the large detuning case, the two eigenstates of the first two eigenvalues span a near-degenerate subspace, and can be considered a pseudo-spin with spin-orbit coupling induced by a gauge potential [10–12]. Under this condition we obtain the effective Hamiltonian [14]

$$H = \frac{p_y^2 + p_z^2}{2m} + v_y\sigma_y p_y + v_z\sigma_z p_z + \gamma_z\sigma_z + V_T, \quad (1)$$

where $v_y = \hbar\kappa_y/m$, $v_z = \hbar\kappa_z\Omega^2/(2m\Delta^2)$, and $\gamma_z = [\hbar^2\Omega^2/(4m\Delta^2)][\kappa_y^2 - (1+\Omega^2/\Delta^2)\kappa_z^2] + \hbar\Omega^2/2\Delta$. Here we have dropped an irrelevant constant and assumed that the potentials $V(\mathbf{r})$ are spin-independent. Furthermore, the atomic gas can well be confined by a 1D optical waveguide along the y axis [13, 14], so we may further restrict our study in the 1D system. We note that compared with the scheme with tripod atomic level configuration [18, 19, 13], here a large detuning is necessary in the Λ-configuration. However, the laser beams are simpler and moreover, the pseudospins in the Λ-configuration would be more robust against the collision of atoms since they are constructed by the lowest two dressed states, while the two dark states in the tripod configuration are usually not the ground states [18, 19, 13].

For 1D cases, the atomic interaction can be described by an effective interacting strength $\widetilde{g} = 4\pi\hbar^2 a_s N/(mV)$, where a_s is the s-wave scattering length, N is the particle number, and V is the effective volume. The interaction between the atoms (per particle) should be much smaller than the confinement frequency (about kHz) [26], and thus it is much smaller than Ω (about MHz). Therefore, the interaction can not pump the atoms outside of the near-degenerate subspace. In addition, we assume that the bosonic atoms are condensed into a Bose–Einstein condensate (BEC) state. Within the Gross–Pitaevskii formalism, the interacting bosons in the near-degenerate subspace are then effectively described by a 1D nonlinear spinor equation $i\hbar\partial_t\Psi = H_{\text{eff}}\Psi$ [27], where

$$H_{\text{eff}} = -\frac{\hbar^2}{2m}\partial_y^2 - i\hbar v_y\sigma_y\partial_y + \gamma_z\sigma_z + \widetilde{g}\Psi^\dagger\cdot\Psi + V_T + V_b, \quad (2)$$

with v_y being the effective speed of light and γ_z as the effective rest energy of the cold atoms. It is a remarkable feature that all parameters, v_y, γ_z, and $\widetilde{g}$, can be controlled experimentally, which provide us a tunable platform to explore the relativistic quantum effects.

With the above spinor Dirac-type equation, we first consider the atomic ZB without nolinear effect, that is $\tilde{g} = 0$. In the Λ-scheme, the atomic dynamics is effectively described by the spinor Hamiltonian (2). We consider the Gaussian wave packet of

$$\Psi(y,0) = \frac{1}{\sqrt{\delta_l\sqrt{\pi}}} e^{ik_0 y} e^{-(y-y_0)^2/2\delta_l^2} \begin{pmatrix} c_1 \\ c_2 \end{pmatrix} \quad (3)$$

as the initial wave function in the spatial space, where $|c_i|^2$ $(i = 1,2)$ normalized as $|c_1^2| + |c_2^2| = 1$ that determines the initial population in the states of $|\chi_i\rangle$, δ_l, k_0, and y_0 are initial wave-packet width, initial averages of wave number and position, respectively. We suppose $\delta_l = \sqrt{\hbar/m\omega_T}$, corresponding to the ground-state width of the trapping potential $\frac{1}{2}m\omega_T^2 y^2$ in y-axis. In the momentum space, the initial wave packet is given by

$$\Phi(k_y,0) = \frac{1}{\sqrt{2\pi}}\int \Psi(y,0)e^{-ik_y y}dy =$$
$$= \frac{1}{\sqrt{\delta_k\sqrt{\pi}}} e^{-i(k_y-k_0)y_0} e^{-(k_y-k_0)^2/2\delta_k^2} \begin{pmatrix} c_1 \\ c_2 \end{pmatrix}, \quad (4)$$

where $\delta_k = \delta_l^{-1}$ is the momentum spread. When $t = 0$, one turns off the trapping potential V_T. The time evolution is governed by Hamiltonian H_{eff} with $V_T = 0$ and $\tilde{g} = 0$, the finial wave function is written as

$$\Psi(y,t) = \hat{\mathcal{T}}\exp\left[-\frac{i}{\hbar}H_{\text{eff}}t\right]\Psi(y,0), \quad (5)$$

where $\hat{\mathcal{T}}$ denotes the time ordering operator. For $V_T = 0$ and $\tilde{g} = 0$, it is straightforward to show that $\Psi(y,t) = \frac{1}{\sqrt{2\pi}}\int \Phi(k_y,t)e^{ik_y y}dk_y$ with

$$\Phi(k_y,t) = \frac{1}{\sqrt{\delta_k\sqrt{\pi}}} e^{-i(k_y-k_0)y_0} e^{-(k_y-k_0)^2/2\delta_k^2} \times$$
$$\times \begin{pmatrix} c_1\cos(\omega_k t) - \frac{v_y k_y c_2 + i\gamma_z c_1/\hbar}{\omega_k}\sin(\omega_k t) \\ c_2\cos(\omega_k t) + \frac{v_y k_y c_1 + i\gamma_z c_2/\hbar}{\omega_k}\sin(\omega_k t) \end{pmatrix}, \quad (6)$$

where $\omega_k = \sqrt{(\gamma_z/\hbar)^2 + (v_y k_y)^2}$ leads to population transfer between two spin states, and thus $\Psi(y,t)$ is sensitive to the initial spinor components.

If we choose $c_1 = c_2 = 1/\sqrt{2}$, the wave packet of atomic gas undergoes ZB. To investigate the atomic ZB, we calculate the expectation value of the center of mass, which is given by

$$\langle y(t)\rangle = i\int dk_y \Phi^\dagger(k_y,t)\partial_{k_y}\Phi(k_y,t) = \\ = y_0 + \frac{v_y\gamma_z}{\hbar\delta_k\sqrt{\pi}}\int dk_y \frac{\sin^2(\omega_k t)}{\omega_k^2} e^{-(k_y-k_0)^2/\delta_k^2}. \quad (7)$$

The integral term stands for ZB which shows the oscillation of the center-of-mass motion. We numerically calculate Eq. (7) and the results are shown in Fig. 2. In the plot, the experiment parameter of Li^7 atomic gas with initial wave number $k_0 = 0$, $k_y = 5.0 \cdot 10^6$ m^{-1}, $m = 1.16 \cdot 10^{-26}$ kg, $\gamma_z^{'} = 10$ kHz, $\delta_l = 10\,\mu$m is chosen. For the sake of convenience, we introduce dimensionless variable scaled by the characteristic length $l_0 = \sqrt{\hbar/m\omega_T} \simeq 10\,\mu$m, energy $E_0/\hbar = \omega_T = 91$ Hz, and time $t_0 = 1/\omega_T \simeq 11$ ms. To get a quantitative intuition, for the above chosen experimental parameters, the minimum amplitude (about 2μm), as shown in Fig. 2c, is readily detectable in current experiment given the fact that the atomic ZB can persist for several milliseconds with frequency of the order of a few KHz. After dimensionless, we get $v_y^{'} = 50$, $\delta_l = 1$, $\gamma_z = 109.93$. Then four different cases are plotted in Fig. 2. The reason for ZB is the separation of initial wave packet by spin and then interfere between the coupling components, which gives rise to oscillation of center-of-mass motion. ZB for finite momentum spread damp out over time, and its lifetime can be increased by reducing momentum spread δ_k. Here, the amplitude of ZB is primarily determined by the central momentum k_0 and the spin-orbit coupling strength v_y'. The smaller k_0 and the larger v_y', the larger amplitude of ZB.

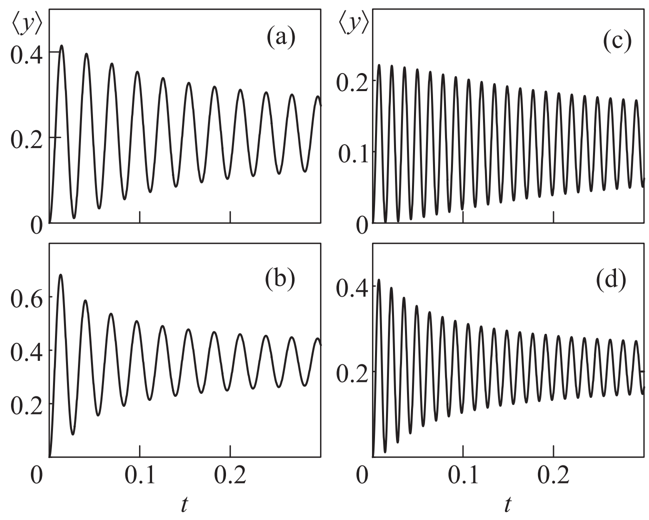

Fig. 2. The ZB with a Gaussian wave packet as an initial state for the wave packet width $\delta = 1$: (a) – $v_y' = 50$ and $\gamma_z = 109.93$, (b) – $v_y' = 100$ and $\gamma_z = 109.93$, (c) – $v_y' = 50$ and $\gamma_z = 219.86$, (d) – $v_y' = 100$ and $\gamma_z = 219.86$

We now turn to investigate the effect of nonlinear interaction on the atomic ZB. Interatomic interaction is crucial in atomic gases which lead to inherent nonlinearity in BEC. At low temperatures, it is dominated by s-wave scattering. Under the mean-field description, an atomic BEC obeys a nonlinear *Schrödinger* equation, the Gross–Pitaevskii (GP) equation, in which the nonlinear strength is proportional to the s-wave scattering length. The strength of nonlinearity can be tuned by Feshbach resonances [28]. The dark and bright solitons have been observed in atomic BECs with repulsive and attractive atom-atom interactions, respectively. Atomic ZB in the nonlinear spinor equation cannot been analytical solved as above. We numerically solve Eq. (5) with $g \neq 0$ by using the split-operator method [29]. When $t = 0$, without atom-laser beams interaction, the BECs is prepared in its ground state. We numerically solve the GP equation using the imaginary time evolution method and obtain the ground state of the condensate. Then we turn off the trapping potential, and meanwhile, we turn on the laser beams, so that the dynamics of the system is governed by 1D nonlinear spinor equation. The position of the atomic center-of mass at time t is given by

$$\langle y(t)\rangle = \int \left[|\Psi_\uparrow(y,t)|^2 + |\Psi_\downarrow(y,t)|^2\right] y dy, \quad (8)$$

where $\Psi_{\uparrow,\downarrow}(y,t)$ can be obtained by numerically solving Eq. (5).

We first consider the case of $g > 0$, which corresponds to the repulsive nonlinear interactions of BECs. Some typical results are shown in Fig. 3, which demonstrates the different nonlinear interaction strengths of atoms with $g = 10, 50, 200$, respectively. From Fig. 3, we find that the larger g, the larger amplitude of ZB. But ZB damps out more quickly and its lifetime is shorter with the increase of repulsive interactions. The reason for this is that in the case of repulsive interactions, the ground state of a BEC is flatter than that in the noninteracting case. So the overlap range of the wave packet is wider, leading to the larger amplitude of the atomic ZB. However, with the increasing of time, due to the repulsive interactions, the wave packet separate more quickly, so that the ZB damp out more quickly with a shorter life time.

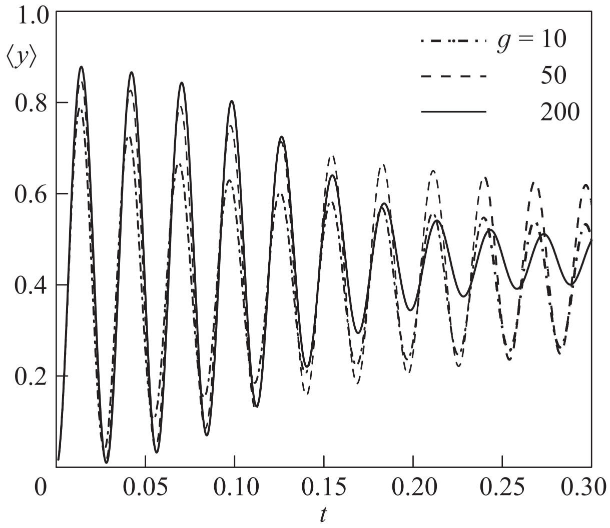

Fig. 3. The ZB under different repulsive nonlinear interaction for $v'_y = 100$ and $\gamma_z = 109.93$. The dashed point line, dashed line and real line correspond to different nonlinear strength

We then consider the case of $g < 0$, which corresponds to the attractive nonlinear interactions of BECs. Fig. 4 shows some typical results of atomic ZB in the at-

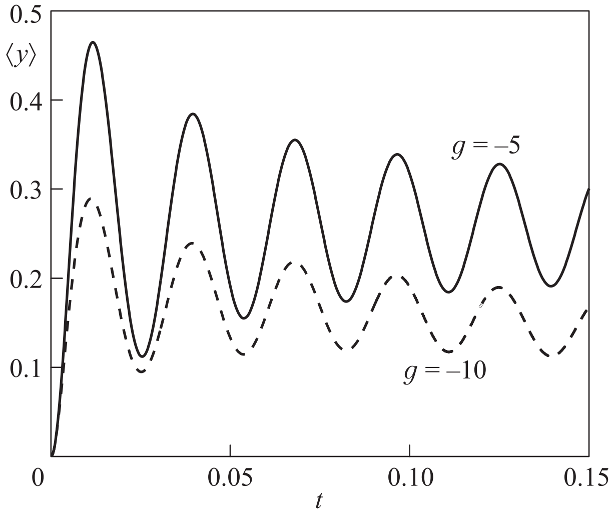

Fig. 4. The ZB under different attractive nonlinear interaction for $v'_y = 100$ and $\gamma_z = 109.93$. The dashed line and real line correspond to different nonlinear strength

tractive interactions case. In this case, we find that in contract, the amplitude of ZB is reduced by the attractive interaction, while the oscillation damps out slower with a longer lifetime as shown in Fig. 4. To see this more clearly, we plotted the atomic ZB of two opposite interactions with the same strength, as shown in Fig. 5. This can be interpreted by the fact that the spatial length

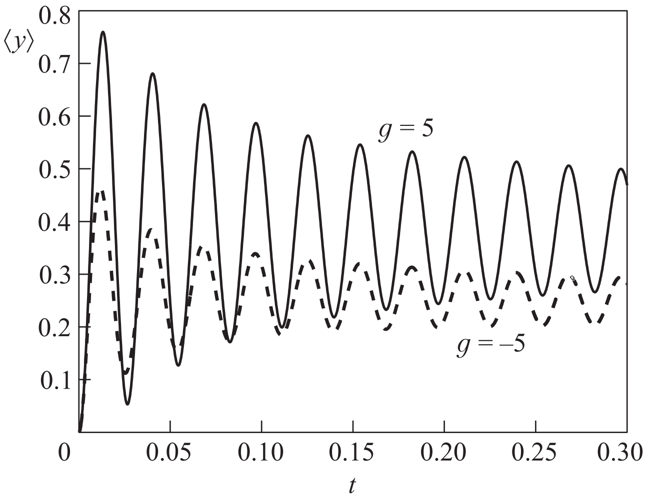

Fig. 5. The ZB under different kinds of nonlinear interaction for $v'_y = 100$ and $\gamma_z = 109.93$. The dashed line and real line correspond to attractive interaction, repulsive interaction, respectively

of the ground state BEC with attritive interatomic interaction is more narrow than that with repulsive interactions. Since the overlap range of the wave packet is narrower, the amplitude of ZB will be smaller. However, increasing time, due to the attractive interactions, the two spin wave packets overlap for a longer time, which gives rise to a longer lifetime of ZB. From the above figures, we can also find that the nonlinear interactions almost have no effect on the frequency of atomic ZB, as the gap between the positive and negative energy states does not change due to the nonlinear interactions.

In conclusion, we have proposed to observe atomic ZB with SO coupled ultracold atoms. We show that large amplitude and long lifetime of ZB can be detectable by tuning laser-atoms interactions in realistic experiment. Based on numerically simulation, the effects of nonlinear interatomic interactions on ZB are investigated. In the repulsive interaction case, the amplitude of ZB is larger, but ZB damps out more quickly with a shorter lifetime. In the attract interaction case, the amplitude of ZB is smaller, but ZB damps out slower with a longer lifetime. However, the nonlinear interactions almost does not affect the frequency of atomic ZB. Considering the fact that the nonlinear interaction is inevitable in atomic gas system, our proposal provide a more realistic situation in simulating the atomic ZB.

This work was supported by the NSFC (# 11004065 and 11104085), the NFRPC (# 2013CB921804), the PCSIRT, and the SRFGS of SCNU.

1. E. Schrödinger and S. P. A. Wiss, Phys. Math. Kl. **24**, 418 (1930).

2. J. Schliemann, D. Loss, and R. M. Westervelt, Phys. Rev. Lett **94**, 206801 (2005).
3. W. Zawadzki, Phys. Rev. B **72**, 085217 (2005).
4. L. Lamata, J. Leon, T. Schatzand, and E. Solano, Phys. Rev. Lett. **98**, 253005 (2007).
5. M. T. Rusin and W. Zawadzki, Phys. Rev. B **76**, 195439 (2007); Phys. Rev. B **80**, 045416 (2009).
6. J. Cserti and G. David, Phys. Rev. B **74**, 172305 (2006).
7. X. Zhang and Z. Liu, Phys. Rev. Lett. **101**, 264303 (2008).
8. X. Zhang, Phys. Rev. Lett. **100**, 113903 (2008).
9. S. Longhi, Opt. Lett. **35**, 235 (2010).
10. J. Ruseckas, G. Juzeliūnas, P. Öhberg, and M. Fleischhauer, Phys. Rev. Lett. **95**, 010404 (2005).
11. S.-L. Zhu, H. Fu, C. Wu, S.-C. Zhang, and L.-M. Duan, Phys. Rev. Lett. **97**, 240401 (2006).
12. X.-J. Liu, M. F. Borunda, X. Liu, and J. Sinova, Phys. Rev. Lett. **102**, 046402 (2009).
13. S.-L. Zhu, D.-W. Zhang, and Z. D. Wang, Phys. Rev. Lett. **102**, 210403 (2009).
14. D.-W. Zhang, Z.-Y. Xue, H. Yan, Z. D. Wang, and S.-L. Zhu, Phys. Rev. A **85**, 013628 (2012).
15. Y. J. Lin, R. L. Compton, A. R. Perry, W. D. Phillips, J. V. Porto, and I. B. Spielman, Phys. Rev. Lett. **102**, 130401 (2009).
16. Y. J. Lin, R. L. Compton, K. Jiménez-García, J. V. Porto, and I. B. Spielman, Nature **462**, 628 (2009).
17. Y. J. Lin, K. Jiménez-García, and I. B. Spielman, Nature **471**, 83 (2011).
18. J. Y. Vaishnav and C. W. Clark, Phys. Rev. Lett. **100**, 153002 (2008).
19. M. Merkl, F. E. Zimmer, G. Juzeliūnas, and P. Öhberg, Europhys. Lett. **83**, 54002 (2008).
20. J. J. Song and B. A. Foreman, Phys. Rev. A **80**, 045602 (2006).
21. Y. P. Zhang, L. Mao, and C. Zhang, Phys. Rev. Lett. **108**, 035302 (2012).
22. D.-W. Zhang, Z. D. Wang, and S.-L. Zhu, Front. Phys. **7**, 31 (2012).
23. Y.-C. Zhang, S.-W. Song, C.-F. Liu, and W.-M. Liu, Phys. Rev. A **87**, 023612 (2013).
24. C. Qu, C. Hamner, M. Gong, C. Zhang, and P. Engels, Phys. Rev. A **88**, 021604(R) (2013).
25. L. J. LeBlanc, M. C. Beeler, K. Jiménez-García, A. R. Perry, S. Sugawa, R. A. Williams, and I. B. Spielman, New J. Phys. **15**, 073011 (2013).
26. D. S. Petrov, G. V. Shlyapnikov, and J. T. M. Walraven, Phys. Rev. Lett. **85**, 3745 (2000).
27. M. Merkl, F. E. Zimmer, and P. Öhberg, Europhys. Lett. **83**, 54002 (2008).
28. C. Chin, R. Girmm, P. Julienne, and E. Tiesinga, Rev. Mod. Phys. **82**, 1225 (2010).
29. M. D. Feit, J. A. Fleck, and A. Steiger, J. Comput. Phys. **47**, 412 (1982).